Volume 11, Number 3 (June 2018) p. 644 – 651 • ISSN 1983-4195
http://dx.doi.org/10.1590/S1983-41952018000300012

REVISTA IBRACON DE ESTRUTURAS E MATERIAIS
IBRACON STRUCTURES AND MATERIALS JOURNAL

Fresh concrete consistency effect on thin-walled columns creep phenomenon

Efeito da consistência do concreto fresco sobre o fenômeno de fluência em pilares parede

E. L. MADUREIRA [a]
edmadurei@yahoo.com.br

L. A. PAIVA [a]
luane_paiva@hotmail.com

Abstract

A concrete structural member when kept under sustained load presents progressive strains over time, associated to the material creep. The fresh concrete consistency, specially, exerts some effect on that phenomenon. The pioneering formulations developed to modelling the creep of concrete are applicable, directly, to the cases for which the stress magnitude remains constant. Its application to reinforced concrete structural members, that exhibits changes in the magnitude of the stresses over such a time dependent phenomenon, requires simplifications from which result the memory models, whose implementation presents the disadvantage of involving the history of the stresses storage. The State Models were developed to overcome these difficulties, as they result of integral calculus scheme improvement, dispensing such computational memory storage. The subject of this work is the analysis of creep strains on reinforced concrete thin-walled columns, emphasizing the fresh concrete consistency efecct, on the base of a state model, fixing the values of its physical parameters from the NBR 6118/14 proceedings [1]. The obtained results showed the occurrence of stresses transfer from the mass of the concrete to the reinforcement steel bars, that was more pronounced in those cases for which the slump test abatement were the highest and, in some cases, including, it induced the material yielding condition.

Keywords: reinforced concrete, thin-walled-column, creep, modelling.

Resumo

Um elemento de concreto, mantido sob tensão de compressão, apresenta contração progressiva no decorrer do tempo, associada à deformação lenta. Em Pilares Parede de concreto armado, as deformações por fluência promovem a transferência de esforços da massa de concreto para as barras da armadura de aço, podendo induzi-las ao escoamento. As formulações pioneiras do efeito de fluência, desenvolvidas com base no coeficiente de fluência, são aplicáveis, sobretudo, quando as tensões se mantêm constantes. Sua aplicação a elementos de concreto armado, por apresentarem variações de tensões no decorrer da manifestação do fenômeno, requer simplificações das quais resultam os modelos de memória, que têm a desvantagem de exigir o armazenamento do histórico de tensões. Os modelos de estado dispensam tal robustez de armazenamento, sendo desenvolvidos a partir do melhoramento do esquema de integração. O objetivo deste trabalho é a análise do efeito de fatores influentes nas deformações por fluência em Pilares Parede de concreto armado, sobretudo, a consistência do concreto fresco, realizada com base em modelo de estado com parâmetros fixados conforme recomendações da NBR 6118/2014.

Palavras-chave: fluência, concreto armado, pilares parede, simulação.

[a] *Universidade Federal do Rio Grande do Norte, Centro de Tecnologia, Departamento de Engenharia Civil, Natal, RN, Brasil.*

Received: 28 Apr 2017 • Accepted: 07 Aug 2018 • Available Online:

1. Introduction

The state of stresses due to sustained load, promotes strains in concrete structural members which progresses over time, characterizing the phenomenon known as creep.

Such kind of strains results, particularly, from the viscous behaviour associated to the adsorbed water layer at the cement grains surface, in the sound concrete (McGregor, 1997), apud [7].

The creep strains are more pronounced in the earlier months of the structure lifetime, when they develop themselves under higher rates. It can endure for periods of time up to five years although it evolves under modest rates over advanced ages.

There are cases for which the creep strains can take magnitudes greater than three times the strains value recorded at the instant of loading, inducing structural displacements of similar extent [8].

Among the relevant factors that influence the creep deformation it may include the moisture content, the stress, the concrete strength, the fresh concrete consistency and the reinforcement ratio.

In the case of reinforced concrete members, the strains due to creep can modify significantly the stresses fields in their constituents elements. In thin-walled columns, specifically, it can promote the stresses reduction on the mass of the concrete and the stresses increase in the reinforcement steel bars, which can induce these latter to experience the yielding phenomenon.

The pioneering formulations for creep deformation modelling were developed from the creep coefficient concept. They are applied, particularly, to structural members for which the stresses on the concrete remain constant over time. Their adequacy for reinforced concrete members, which exhibit stresses variations during the creep phenomenon, depends on the application of simplifier artifices that result on memory models. These kinds of formulations are so named because they demand, in its calculation, the history of stresses storage, resulting in large-scale storage amount that can become the modelling unfeasible. In order to overcome the difficulties related to such a computational memory storage, it was developed the state models, from the integrating scheme changing, that provide the use, exclusively, of the stresses at the previous discrete instant of time from that one considered.

The aim of this work is the simulation of the creep strain on reinforced concrete thin-walled columns, based on a state model, whose parameters were fixed from the NBR 6118/14 proceedings [1], focused, above all, to the analysis of the fresh concrete consistency effect upon the analysed phenomenon.

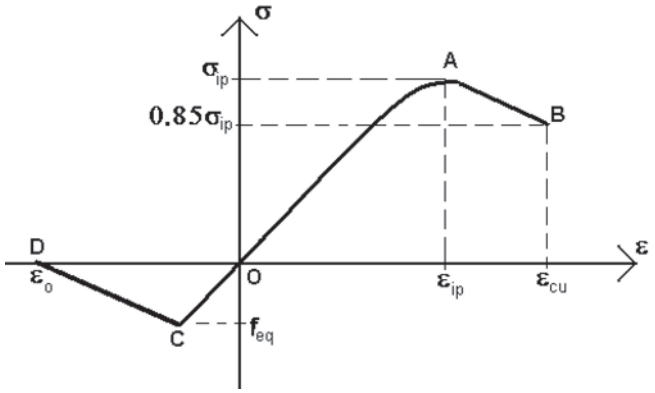

Figure 1
Stress strain curve for the concrete

2. Modelling

In this analysis work the quadratic isoparametric finite elements approximation was adopted.

2.1 Concrete response to loading

The analysis was carried out by the use of an orthotropic nonlinear framework proposed by Kwak and Filippou [6] in plane state of stress, on incremental iterative procedure and the finite element approach. The constitutive matrix elements were defined through equations similar to those employed in uniaxial state of stress, however, taking as a reference, the equivalent deformations "ε_{ei}", that, for every principal directions, are given by:

$$\varepsilon_{ei} = \varepsilon_i + D_{ij}\varepsilon_j / D_{ii} \quad (1)$$

The "i" and "j" indexes refer to principal plane direction. The "D_{ij}" coefficients represent the constitutive matrix elements.

The concrete in compression mechanical performance was simulated from the constitutive relationships proposed by Hognestad [2], presented in the form:

$$\sigma_i = \frac{2\sigma_{ip}}{\varepsilon_{ip}}\left(1 - \frac{\varepsilon_{ei}}{2\varepsilon_{ip}}\right)\varepsilon_{ei}, \text{ for } \varepsilon_{ip} < \varepsilon_{ei} < 0 \quad (2)$$

The "σ_{ip}" and "ε_{ip}" parameters represent the concrete peak stress and its corresponding strain, beyond every principal direction namely "i". The "ε_{cu}" parameter, in turn, is the concrete ultimate strain in uniaxial compression. Equation 2 represents the hardening branch, the OA segment on the curve of figure 1.

In this work, as recommended by [1], the secant modulus, "E_c", was adopted, and is given by:

$$E_c = 0.85E_o = 0.85 \times 5600\sqrt{f_{ck}} = 4760\sqrt{f_{ck}} \quad (3)$$

Where the "E_o" parameter is the concrete initial deformation modulus and the "f_{ck}" parameter is the concrete characteristic compressive strength.

The concrete ultimate stresses are defined from the failure envelope proposed by Kupfer and Gerstle [5], figure 2, whose analytical representation in biaxial compression state is:

$$(\beta_1 + \beta_2)^2 - \beta_2 - 3.65\beta_1 = 0 \quad (4)$$

Where $\beta_i = \frac{\sigma_{ip}}{f_c}$. The parameter "$f_c$" is the concrete uniaxial compressive strength. Letting $\alpha = \sigma_1/\sigma_2$ where the σ_1 and σ_2 parameters are the principal stresses such that $0 > \sigma_1 > \sigma_2$, from the equation 4 results:

$$\sigma_{2c} = \frac{1 + 3.65\alpha}{(1 + \alpha)^2} f_c \text{ and } \sigma_{1c} = \sigma_{cu} = \alpha\sigma_{2c} \quad (5)$$

The strains related to peak stresses in biaxial compression state,

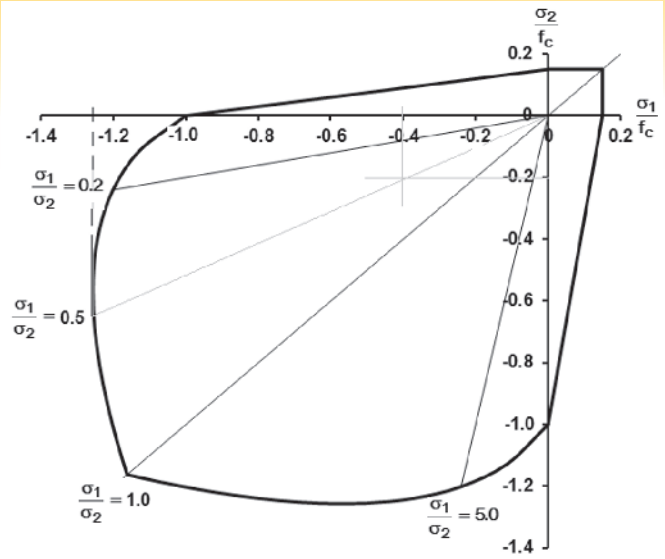

Figure 2
Ultimate stress envelop for concrete in biaxial state of stresses

"ε_{2p}" and "ε_{1p}", according to [6], are obtained from the expressions:

$$\varepsilon_{2p} = \varepsilon_{co}(3\beta_2 - 2) \quad \text{and} \quad \varepsilon_{1p} = \varepsilon_{co}(-1.6\beta_1^3 + 2.25\beta_1^2 + 0.35\beta_1) \tag{6}$$

For which the "ε_{co}" parameter is the deformation corresponding to the stress peak compression in uniaxial state of stress.
The constitutive relationship on an incremental fashion proposed by Desai and Siriwardance (apud [6]), to modeling the biaxial state of stress concrete mechanical behavior, was adopted. It is expressed by:

$$\begin{vmatrix} d\sigma_1 \\ d\sigma_2 \\ d\tau_{12} \end{vmatrix} = \frac{1}{1-\nu^2} \begin{vmatrix} E_1 & \nu\sqrt{E_1E_2} & 0 \\ \nu\sqrt{E_1E_2} & E_2 & 0 \\ 0 & 0 & (1-\nu^2)G \end{vmatrix} . \begin{vmatrix} d\varepsilon_1 \\ d\varepsilon_2 \\ d\gamma_{12} \end{vmatrix} \tag{7}$$

On equation 7, "$d\sigma_1$", "$d\sigma_2$" e "$d\tau_{12}$" are the stress increments through the principal directions. The "E_i's" parameters are the concrete tangent deformation modules relating to such directions and "v" is the concrete Poisson's ratio. The "**G**" parameter is the concrete transverse deformation module that is obtained from the relationship:

$$(1-\nu^2)G = 0.25(E_1 + E_2 - 2\nu\sqrt{E_1E_2}) \tag{8}$$

To represent the mass of concrete region, the plane eight-nodded quadrilateral elements Q8, figure 3.a, was used.

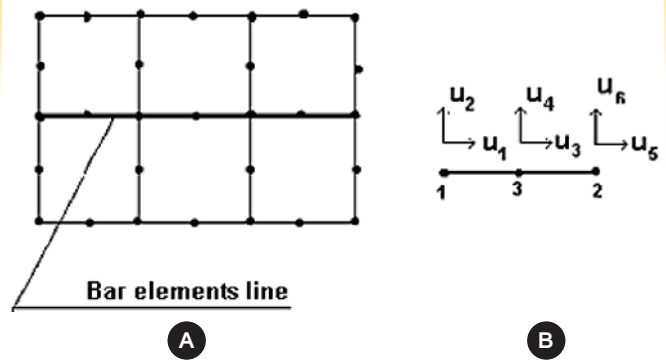

Figure 3
Finite elements: a) Plane Q8; b) bar L3

2.2 Steel response to loading

The steel behaviour is considered as elastic perfectly plastic. Due to the great transverse flexibility of the reinforcement steel bars, only axial stiffness is considered in its mechanical performance, and then they are simulated by bar three-nodded elements L3, figure 3.b. In this way, the related stiffness matrix "K" is expressed by:

$$K = \frac{2AE}{L}\begin{bmatrix} 1 & 0 & -1 \\ 0 & 1 & -1 \\ -1 & -1 & 2 \end{bmatrix} \tag{9}$$

where the "E" parameter represents the steel Young's modulus, which is considered equal to 210 GPa. "A" is the reinforcement cross sectional area, while "L" represents the bar finite element length.

2.3 Creep strains

The creep strains, "$\varepsilon_c(t)$", are simulated from the state model proposed by Kawano and Warner [4], expressed on the form:

$$\varepsilon_c(t) = \varepsilon_{cd}(t) + \varepsilon_{cv}(t) \tag{10}$$

Where "$\varepsilon_{cd}(t)$" and "$\varepsilon_{cv}(t)$" are the deformations parcels due to hardening and visco-elastic effects, respectively, defined as:

$$\varepsilon_{cd}(t) = -\frac{1}{E_o}\int_0^t \frac{d\phi_d(t,\tau)}{d\tau}\sigma(\tau)d\tau \quad \text{and}$$
$$\varepsilon_{cv}(t) = -\frac{1}{E_o}\int_0^t \frac{d\phi_v(t,\tau)}{d\tau}\sigma(\tau)d\tau \tag{11}$$

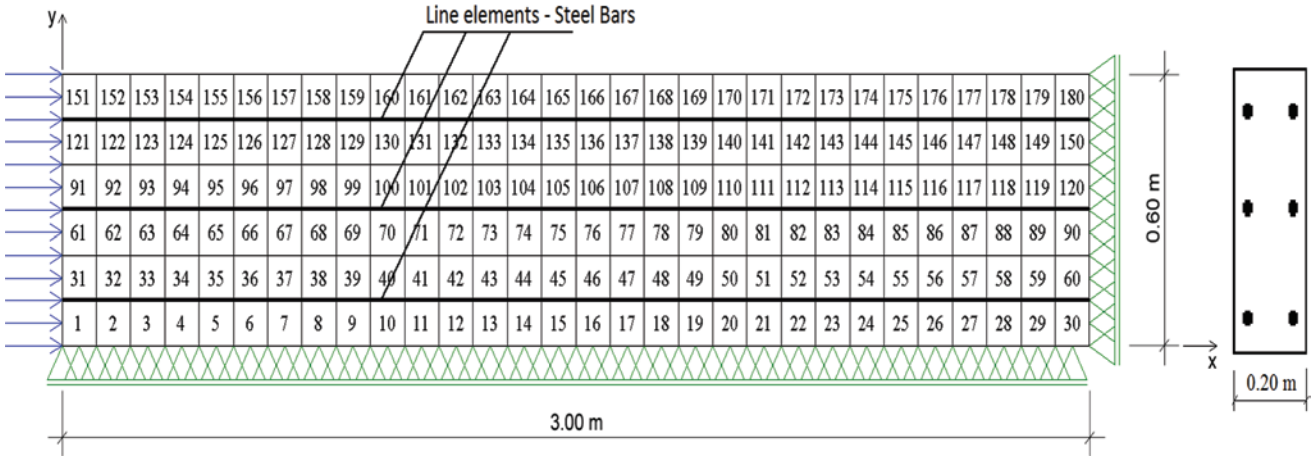

Figure 4
Basic model, problem domain and finite element mesh

In which the "$\phi_d(t,\tau)$" and "$\phi_v(t,\tau)$" functions represent their respective creep coefficients. In their incremental versions these parcels are presented in the form:

$$\Delta\varepsilon_{cd}(t_n) = \frac{1}{E_o}\sigma(t_{n-1})\left[\phi_d(t_n,t_o) - \phi_d(t_{n-1},t_o)\right] \quad (12)$$

and,

$$\Delta\varepsilon_{cv}(t_n) = \left[\frac{\phi_v^*}{E_o}\sigma(t_{n-1}) - \varepsilon_{cv}(t_{n-1})\right]\left(1 - e^{-\Delta t_n/T_v}\right) \quad (13)$$

For which:

$$\phi_d(t_n,t_o) = \frac{(t_n - t_o)^{0.6}}{10 + (t_n - t_o)^{0.6}}\phi_d^* \text{ and} \quad (14)$$

$$\phi_v(t_n,t_j) = \left[1 - e^{-(t_n - t_j)/T_v}\right]\phi_v^*$$

Where "ϕ^*_d" and "ϕ^*_v" are the asymptotic creep coefficient for those two parcels, and "T_v" is the retardation time. "t_n" is the instant for which the creep deformations are being calculated, "t_{n-1}" is the discrete instant, immediately preceding the instant "t_n", and "t_o" is the concrete age at the instant of loading. At every instant "t_n" the creep strains are described according:

$$\varepsilon_c(t_n) = \varepsilon_c(t_{n-1}) + \Delta\varepsilon_c(t_n) \quad (15)$$

Such that "$\Delta\varepsilon_c(t_n)$" is the incremental creep strain and is obtained from:

$$\Delta\varepsilon_c(t_n) = \Delta\varepsilon_{cd}(t_n) + \Delta\varepsilon_{cv}(t_n) \quad (16)$$

It is assumed that, during every time interval, the stresses magnitudes remain constant, although, they present some variation over all the phenomenon observation period under a step kind function.

3. Computational support

With a view to the acquisition of the results aimed at the fulfilment of the objectives of this work, it was employed the software named "Análise Constitutiva Não-Linear" – ACNL [7]. Such program was structured according to incremental and iterative procedure and the Finite Elements Method (FEM), on a Nonlinear Orthotropic Formulation in plane state of stresses[6]. It even covers, in its algorithmic framework, the element formulations described in the item 2 of this paper.

4. Program validation

For its validation purpose, the program was used to analyze, in a plane state of stresses, a rectangular cross-sectional concrete thin-walled column that is 3.00 m height, 0.20 m thick and 1.20 m width, figure 4, considering, specially, the cases 1 and 7, whose concrete slump test abatement, reinforcement ratio, load and moisture content are described in table 1. The results of such analysis were compared with their corresponding values obtained by use of a simplified model, drawn up on the basis of the Solid Mechanic Postulates, in the uniaxial state of stresses, as

Table 1
Studied cases characterization

Cases	Slump (cm)	Reinforcement ratio (%)	Load (kn)	Moisture content (%)	ϕ^*v
1	0 - 4	0.63	3750	40	0.89
2	0 - 4	0.63	3750	60	0.35
3	0 - 4	0.63	3750	80	0.00
4	0 - 4	1.00	3900	40	0.89
5	0 - 4	1.00	3900	60	0.35
6	0 - 4	1.00	3900	80	0.00
7	0 - 4	1.58	4152	40	0.89
8	0 - 4	1.58	4152	60	0.35
9	0 - 4	1.58	4152	80	0.00
10	5 - 9	0.63	3750	40	1.63
11	5 - 9	0.63	3750	60	0.92
12	5 - 9	0.63	3750	80	0.15
13	5 - 9	1.00	3900	40	1.63
14	5 - 9	1.00	3900	60	0.92
15	5 - 9	1.00	3900	80	0.15
16	5 - 9	1.58	4152	40	1.63
17	5 - 9	1.58	4152	60	0.92
18	5 - 9	1.58	4152	80	0.15
19	10 - 15	0.63	3750	40	2.36
20	10 - 15	0.63	3750	60	1.48
21	10 - 15	0.63	3750	80	0.53
22	10 - 15	1.00	3900	40	2.36
23	10 - 15	1.00	3900	60	1.48
24	10 - 15	1.00	3900	80	0.53
25	10 - 15	1.58	4152	40	2.36
26	10 - 15	1.58	4152	60	1.48
27	10 - 15	1.58	4152	80	0.53

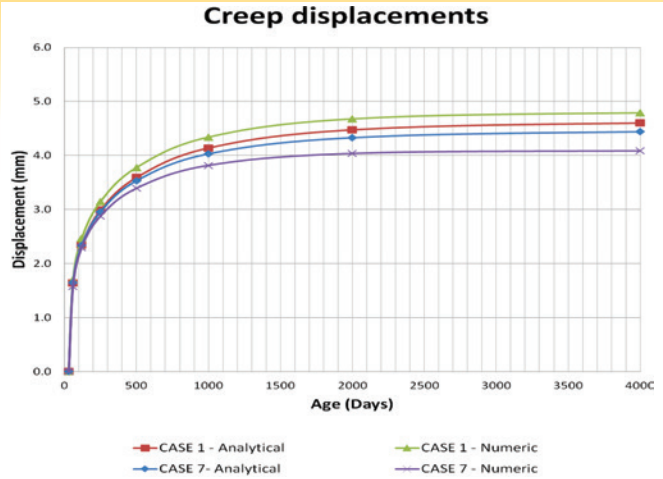

Figure 5
Creep displacements by time curves

performed by Madureira at al [8]. The obtained results showed a good agreement, Figure 5.

5. Analysed models

The studied models are rectangular cross-sectional concrete thin-walled column, 3.00 m height, 0.20 m thick and 1.20 m width, cast in C 40 concrete, reinforced by CA-50 steel bars, figure 4.

The structural member is subjected to a uniform load that is distributed on the top section, whose magnitude progresses on a gradual way from zero to a final value fixed at about 40% of that value corresponding to concrete ultimate compressive stress, table 1, according the limitations, in terms of stresses, of the NBR 6118/14 proceedings creep model [1].

The analysis was performed on twenty-seven cases, differentiated among themselves by the slump test abatement, by the reinforcement ratio and by the moisture content, as shown in columns 2, 3 and 5, respectively, on table 1.

Due to the symmetry of the problem, its domain, on the "xy" plane, could be defined from the rectangular area whose horizontal dimension is equal to the column height, and the vertical dimension is equal to its half width, and its discretization was performed on the basis of plane and bar elements, both 0.10 m length, resulting the mesh composed by 180 plane elements and 90 bar elements, figure 4. It is observed that in all column figures the structural member is being represented with its longitudinal axis coinciding with the "x" direction.

The age of the concrete at the instant of loading was set as 30 days. It was considered that the overall column surface perimeter is exposed to the environment medium. The retardation time was fixed as Tv = 600 days. The asymptotic hardening creep coefficient was considered as being $\phi_d^* = 2.0$, as recommended by Kawano and Warner [4]. The asymptotic creep coefficient related to viscous elastic effects, ϕ_v^*, exhibit distinct values, case to case, as shown in column 6, table 1, that is obtained by the difference between the total asymptotic creep coefficient of NBR 6118/2014 [1] and the asymptotic hardening creep coefficient.

The analysis was performed according to the "Plane State of Stresses".

For the purposes of covering the creep phenomenon longevity, the maximum age limit of concrete was set as 4000 days, which corresponds to the age from which the creep displacements, virtually, stabilizes, figure 5. Such a period of time was discretized from observation instants at 60, 120, 250, 500, 1000, 2000 and 4000 days.

6. Results and discussion

From the obtained results it may be observed that, for the equilibrium configuration referring to the final load, the fields of the axial displacements and of the normal stresses took the morphologies shown in figures 6 and 7, respectively. For all studied cases, the displacement magnitude at the column top and the stress on the mass of the concrete, were about 2.1 mm and 15 MPa, respectively, table 2.

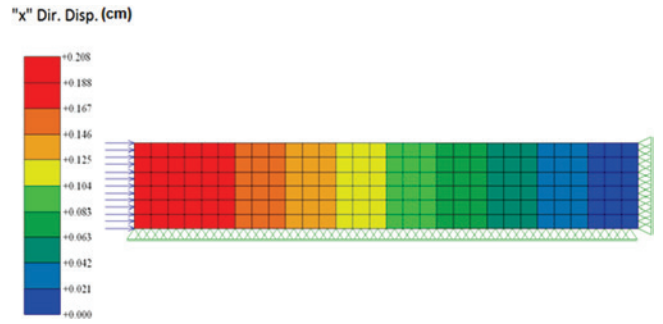

Figure 6
Field of axial displacement at the instant of loading – Case 16

Figure 7
Field of normal stresses at the instant of loading – Case 16

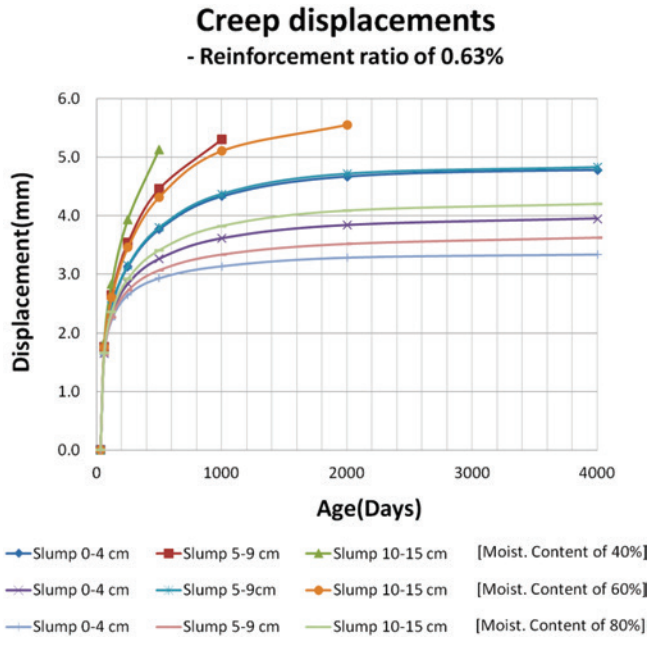

Figure 8
Creep displacement curves for reinforcement ratio of 0.63%

Table 2
General results

Cases	Displacement (mm)		Concrete stress (MPa)		Reinforcement stress (MPa)	
	Loading	Creep	Loading	Creep	Loading	Creep
1	2.05	4.83	14.8	12.6	143.3	479.6
2	2.05	4.02	14.8	13.0	143.3	423.0
3	2.05	3.46	14.8	13.2	143.3	384.2
4	2.07	4.51	14.9	11.6	144.3	456.8
5	2.07	3.80	14.9	12.2	144.3	408.2
6	2.07	3.30	14.9	12.6	144.3	373.8
7	2.10	4.10	15.0	10.0	146.4	428.4
8	2.10	3.53	15.0	11.1	146.4	389.6
9	2.10	2.80	4152	80	0.00	0.00
10	2.05	5.96	14.8	12.8	143.3	500.0
11	2.05	4.88	14.8	12.6	143.3	482.6
12	2.05	3.70	14.8	13.1	143.3	401.0
13	2.07	5.37	14.9	11.3	144.3	500.0
14	2.07	4.55	14.9	11.6	144.3	459.4
15	2.07	3.55	14.9	12.4	144.3	388.9
16	2.10	4.76	15.0	9.6	146.4	472.2
17	2.10	4.13	15.0	10.4	146.4	430.5
18	2.10	3.29	15.0	11.4	146.4	373.6
19	2.05	7.13	14.8	12.5	143.3	500.0
20	2.05	5.55	14.8	12.5	143.3	500.0
21	2.05	4.26	14.8	12.9	143.3	440.2
22	2.07	6.23	14.9	11.4	144.3	500.0
23	2.07	5.21	14.9	11.4	144.3	500.0
24	2.07	4.05	14.9	12.0	144.3	425.0
25	2.10	5.49	15.0	9.9	146.4	500.0
26	2.10	4.64	15.0	9.8	146.4	464.1
27	2.10	3.73	15.0	10.9	146.4	403.3

By examining the field of stresses, figure 7, it may be noted that the overall feature shows discrete stress variations, except on the region near of the column top, namely the loading introduction zone, where a tenuous disturbance was raised.

Once the creep phenomenon has been triggered, the strains by time evolved according the curves showed in figure 8. It may be observed that, as the softest the fresh concrete consistency as the greatest column displacements. For some studied cases it occurred the yielding phenomenon in the steel reinforcement bars even before the creep stabilization, that's why, the associated curves in figure 8 are interrupted before 2400 days. For case 25, specially, the field of creep displacements stabilised itself at 4000 days according the fashion presented in figure 9. For the remaining cases, up to the age for which the mechanical analysis has carried

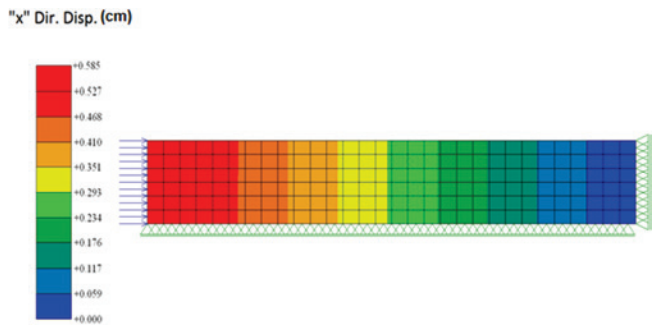

Figure 9
Longitudinal displacement field due to creep at 4000 days – Case 25

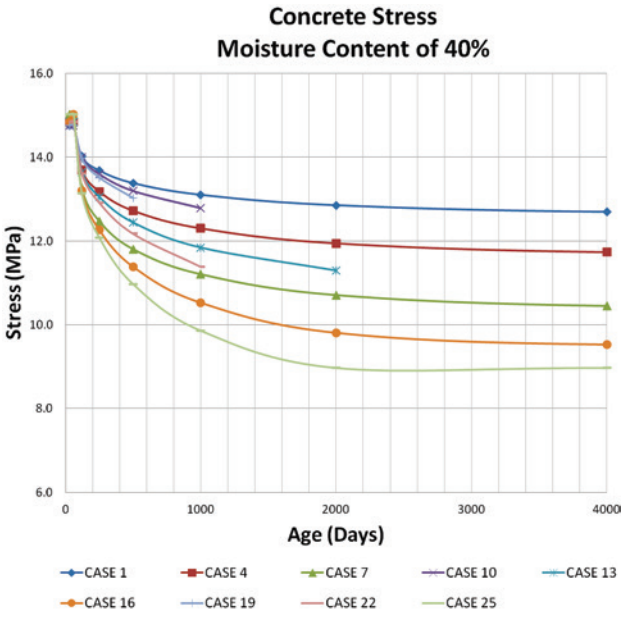

Figure 10
Evolution of stresses on the concrete for 40% moisture content

Figure 11
Normal stress field in the concrete at 4000 days – Case 16

out, the field of creep displacements presented similar features differentiated, solely, by their numeric values, table2. The smallest increase of creep displacements was registered for case 9, which refers to the smallest slump test abatement. The magnitude of such a displacement was about 2.8 mm, corresponding to 1.3 times the displacement at the instant of loading. The largest increase of creep displacements, in the other hand, was registered for case 19, which concerning to the highest slump test abatement, reaching a magnitude about 7.1 mm, that corresponds to 3.5 times the displacement at the instant of loading.

Due to creep strains the mass of the concrete experienced stress relief. The stress magnitudes evolved in accordance to the curves of figure 10. For case 16 the stresses field stabilised itself according the aspect illustrated in figure 11. For the other cases, the fields of stresses display similar fashion, differing mainly with regard to the stresses magnitudes, table 2. The lowest stress relief was about 10%, registered in case 3, that is referred, to the lowest slump test abatement while one of the largest stress relief was about 35%, verified to the case 26, referring to the highest slump test abatement. It is observed from the comparison between figures 7 and 11 that the creep strains have intensified the stresses disturbance at the column top region.

As a result of the creep effect the stresses on the reinforcement steel bars evolved according the curves of figure 12, noting up their magnitude increase. The smallest overstress was registered to the case 9, referring to the lowest slump test abatement, whose variation was about 164%, table 2. On the other hand, the largest one was observed in cases 19, 20, 22, 23 and 25, referring to the highest slump test abatement culminating, acording table 2, in the material yielding, in some cases, already, after 500 days from the concrete cast.

The fresh concrete consistency effect upon the concrete sound creep strains is enhanced from the curves of figure 13. The obtainned results reveal that, for the crescent range by the slump test abatement from 0 to 4 cm, from 5 to 9 cm and from 10 to 15 cm, the effective creep coefficient, that is defined as the ratio between the column shortening due to creep and its value registered at the instant of loading, presented the crescent values 2.4, 2.9 and 3.5, resulting on a difference of aproximatilly 47%, between the largest and the smallest values for such parameter.

7. Conclusions

This work refers to the analysis of the fresh concrete consistency effect upon creep strains on reinforced concrete thin-walled columns, on the basis of a state model, from a non-linear orthotropic formulation and the finite element approximation.

In order to the fulfilment this subject, some cases differentiated among themselves by the slump test abatement, by the reinforcement ratio and by the moisture content were studied

The obtained results showed that for the adopted values by environmental conditions and the parameters of the analysed cases, the creep strains, virtually, reaches the stationary condition before

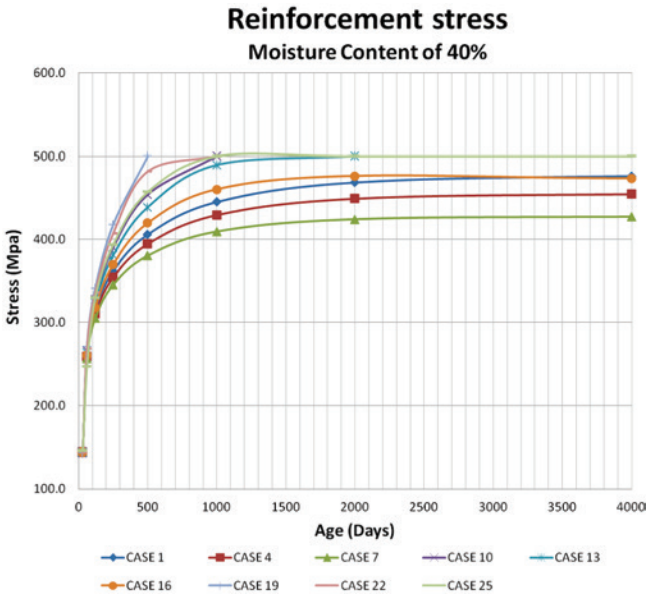

Figure 12
Evolution of stresses on the reinforcement for 40% moisture content

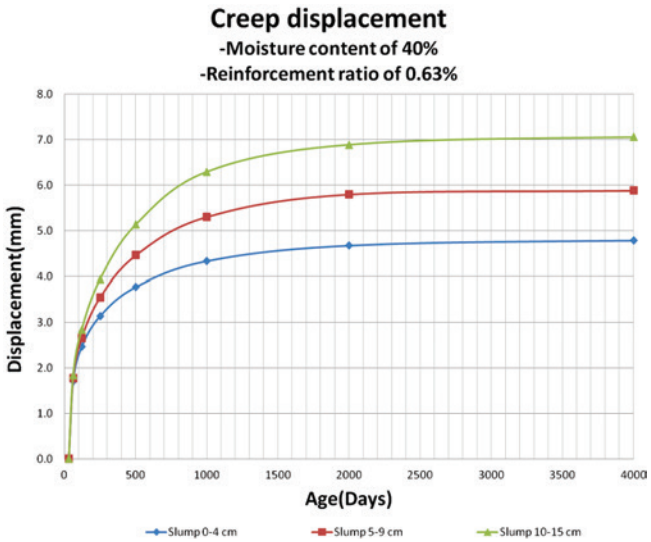

Figure 13
Creep displacements according the concrete consistency

the age of 4000 days from concrete cast.
Furthermore, it was noted the occurrence of stresses relief in the mass of concrete that was as greater as higher the slump test abatement, as it would be the expected trend.
The analysis performed in this paper pointed out too, the occurrence of stresses increase on the reinforcement steel bars as yeah reported in [3] that, for some of the highest slump test abatement cases, culminated with the material yielding condition, as reported in [8], already, at 500 days from the concrete cast.
In addition, it was observed that, the effective creep coefficient, defined as the ratio between the column shortening due to creep and the observed contraction at the instant of loading, assumed values as greater as higher the slump test abatement, enhancing in this way that, as softer the fresh concrete consistency the larger the creep strains.
It is worthwhile to mention that, in some of those studied cases whose slump test abatement was the highest, the creep strains at earlier ages were so pronounced that the steel of the reinforcement bars reached the yielding condition too precociously and so the column lost its structural stability before the concrete creep strains had reached the stationary stage. In this way, as a matter of fact, the concrete creep displacements presented values much lower than it would have been if still yelding had not occurred so early.

8. Acknowledgements

This report is part of a research work on the numerical simulation of the creep strains on reinforced concrete members supported by the Fundação Coordenação de Aperfeiçoamento de Pessoal de Nível Superior – CAPES and by the Pró-Reitoria de Pesquisa da Universidade Federal do Rio Grande do Norte – UFRN. Their support is gratefully acknowledged.

9. References

[1] ASSOCIAÇÃO BRASILEIRA DE NORMAS TÉCNICAS. NBR 6118: Projeto de Estruturas de Concreto - Procedimento. Rio de Janeiro: ABNT, 2007.

[2] HOGNESTAD, E. A Study of Combined Bending and Axial Load in Reinforced Concrete Members. University of Illinois, Engineering Experiment Station, Bolletin n. 399, Urbana, Illinóis, Vol. 49, n 22, 1951.

[3] KATAOTA, L.T.; MACHADO, M.A.S.; BITTENCOURT, T.N. Análise Numérica da Transferência de Carga do Concreto para a Armadura em Pilares de Concreto Armado Devida à Fluência e Retração. In: CONGRESSO BRASILEIRO DE CONCRETO, 52, 2010. Fortaleza. Anais… Fortaleza: IBRACON, 2010.

[4] KAWANO, A.; WARNER, R.F. Model Formulations for Numerical Creep Calculations for Concrete. Journal of Structural Engineering, [S.l.], vol. 122, n. 3, p. 284-290, 1996.

[5] KUPFER, H.B.; GERSTLE, K.H. Behaviour of Concrete under Biaxial Stresses. Journal of Engineering Mechanics, [S.l.], vol. 99, n. 4, p. 853-866, 1973.

[6] KWAK, H.G.; FILIPPOU, F.C. Finite Elements Analysis of Reinforced Concrete Structures Under Monotonic Loads. Report UCB/SEMM-90/14, Berkeley, Califórnia, 1990.

[7] MADUREIRA, E.L. Simulação Numérica do Comportamento Mecânico de Elementos de Concreto Armado Afetados pela Reação Álcali-Agregado. 2007. Tese (Doutorado em Engenharia Civil) – Departamento de Engenharia Civil - Universidade Federal de Pernambuco, Recife, 2007.

[8] MADUREIRA, E.L., SIQUEIRA, T.M. and RODRIGUES, E.C. Creep Strains on Reinforced Concrete Columns. IBRACON Structural and Material Journal, Vol. 6, n.4, p. 537-560, 2013.